

Order Statistics-based Design of UWB Receivers

*Original*

Order Statistics-based Design of UWB Receivers / Badawy, Ahmed; Elfouly, Tarek; Khattab, Tamer; Chiasserini, Carla Fabiana; Trincherò, Daniele. - In: IEEE WIRELESS COMMUNICATIONS LETTERS. - ISSN 2162-2337. - STAMPA. - 9:9(2020), pp. 1427-1431. [10.1109/LWC.2020.2992902]

*Availability:*

This version is available at: 11583/2818912 since: 2020-09-10T11:33:15Z

*Publisher:*

IEEE

*Published*

DOI:10.1109/LWC.2020.2992902

*Terms of use:*

This article is made available under terms and conditions as specified in the corresponding bibliographic description in the repository

*Publisher copyright*

IEEE postprint/Author's Accepted Manuscript

©2020 IEEE. Personal use of this material is permitted. Permission from IEEE must be obtained for all other uses, in any current or future media, including reprinting/republishing this material for advertising or promotional purposes, creating new collecting works, for resale or lists, or reuse of any copyrighted component of this work in other works.

(Article begins on next page)

# Order Statistics-based Design of UWB Receivers

Ahmed Badawy, *Member, IEEE*; Tarek Elfouly, *Senior Member, IEEE*; Tamer Khattab, *Senior Member, IEEE*; Carla Fabiana Chiasserini, *Fellow, IEEE* and Daniele Trincherò, *Member, IEEE*

**Abstract**—We propose a non-coherent ultra-wideband (UWB) receiver that leverages a single-sample-per-pulse threshold approach to detect the transmitted symbol and is capable of mitigating the impact of impulse interference. Unlike classical detectors, the proposed receiver does not aim for the peak ( $1^{st}$ -order) sample, rather it selects the optimal  $\ell^{th}$ -order one over the samples of a single pulse. We derive the error probability both under additive white Gaussian noise, for which a closed-form expression is obtained, and under the IEEE 802.15.4a channel model. We also conduct extensive simulations and show that the proposed solution significantly outperforms both single peak and energy detection UWB receivers in the presence of impulse interference.

**Index Terms**—UWB, non-coherent receiver, pulse detection

## I. INTRODUCTION

A well-known method for implementing non-coherent UWB receivers is energy detection (ED) [1], [2]. The ED approach has low implementation complexity, although its performance is sensitive to varying background noise and interference levels. Due to the peculiarity of UWB systems, the symbol time is usually much larger than the duration of the transmitted short pulse. This, in addition to the channel delay spread, leads to a stringent requirement on the pulse duration tuning window. Otherwise, noise-only samples are collected, yielding a higher noise floor and, hence, a severe degradation of the performance of ED-based UWB receivers. Other relevant examples of non-coherent UWB receivers leveraging single sample-based detection are single- and dual-peak receivers, as discussed in [3]. In single sample-based UWB receivers, the peak sample is selected from the received signal and then compared against a threshold to decide whether a “1” or “0” was transmitted. The performance of such receivers is close to that of ED-based receivers.

One of the main issues in the reception of UWB signals is impulsive interference (IN), which affects many communication scenarios such as industrial and underwater environments (see, e.g., [4]–[6], and the references therein). To effectively cope with IN, [5], [7]–[9] have proposed UWB receivers that account for this phenomenon, exploiting non-linear and sparsity based methods. All these solutions require high processing capabilities and perfect channel estimation at the receiver, and yet the performance is sub-optimal [6]. Another possible approach is to apply a simple clipping at the receiver’s analog

front-end. However, the threshold should be set higher than the maximum desired signal amplitude, otherwise the desired signal will be clipped and lead to high error rates. This leaves a large gap for IN to pass the threshold and impact the receiver, ultimately yielding just a slight improvement in performance. Moreover, since the UWB signal is non-uniformly distributed within the received symbol time, existing non-linear high processing receivers [8], [9] turn out to be sub-optimal under IN [6].

In this paper, we propose a UWB non-coherent receiver based on single-sample thresholding, which exhibits a significantly lower error rate than existing non-coherent receivers in the presence of IN. Our approach is based on sorting the received samples based on their amplitude, and on selecting the  $\ell^{th}$ -order sample to be compared against a threshold, which minimizes the error probability. If the value of the selected sample exceeds the threshold, a “1” is detected; otherwise, a “0” is output. Importantly, our proposed receiver does not require tuning to the pulse duration, rather it operates on the entire symbol time. We analyse the performance of the proposed receiver, first under Gaussian noise obtaining a closed-form expression for the error probability, and the under a fading channel. Through simulations under the IEEE 802.15.4a channel model, we also compare the performance of our receiver versus single-peak and ED solutions and show its superiority.

The rest of the paper is organized as follows. Sec. II introduces the system model under study, while Sec. III presents the proposed receiver design and its performance analysis aimed at deriving an expression for the error probability. Sec. IV discusses the numerical results and the comparison against existing techniques. Finally, Sec. V concludes the paper.

## II. SYSTEM MODEL

We consider UWB communications leveraging on-off Keying (OOK) modulation, where symbols  $d_k \in \{0, 1\}$  are transmitted over a sequence of ultra-short pulses,  $p$ , each of pulse duration  $T_p$ . The transmitted OOK UWB signal can be written as [10]

$$s(t) = \sum_k d_k p(t - kT_R), \quad (1)$$

where  $T_R \gg T_p$  is the symbol duration and  $R = 1/T_R$  is the symbol rate. We assume that the symbol time is much longer than the delay spread, which leads to zero inter-symbol interference. It is also assumed that the transmitter and the receiver are synchronized.

This publication was made possible by the support of the NPRP grant 7-923-2-344 from the Qatar National Research Fund (QNRF). The statements made herein are solely the responsibility of the authors.

A. Badawy, C. F. Chiasserini and D. Trincherò are with Politecnico di Torino, Italy (ahmed.badawy, daniele.trincherò, chiasserini@polito.it). T. Elfouly is with the Department of Computer Engineering at Qatar University (tarekfouly@qu.edu.qa) and T. Khattab is with the Department of Electrical Engineering at Qatar University, Doha, Qatar (tkhattab@ieee.org).

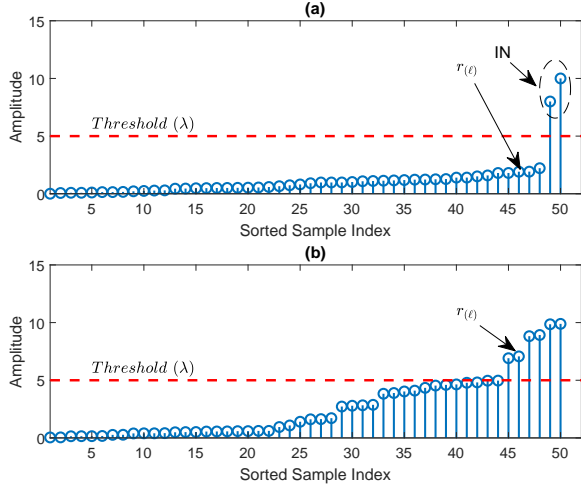


Fig. 1: Example of the impact of IN: (a): when “0” is transmitted and (b) when “1” is transmitted.

### III. RECEIVER DESIGN AND PERFORMANCE ANALYSIS

The rationale behind our receiver design is as follows. Let us first sort the samples collected in each symbol time, in ascending order as depicted in Fig. 1 (a similar procedure holds if they are sorted in a descending order). When sending a “0”, the receiver collects noise-only samples and, in the presence of IN, the last few sorted samples with highest amplitudes are affected by the interference. It follows that a “0” transmission would be better detected if one of the samples ( $r_{(\ell)}$ ) other than the peak is selected and compared to the pre-set threshold ( $\lambda$ ), as it would result below threshold with higher probability. On the contrary, when a “1” is sent,  $r_{(\ell)} > \lambda$  implies that all samples with index higher than  $\ell$  are also above threshold, which makes the detection of the “1” more reliable. In a nutshell, in order to reduce the impact of IN and, hence, improve the detection performance, our solution selects the sample with the order (index) that minimizes the error probability and compares this sample against the preset threshold. More specifically, the optimal sample order is obtained by solving the following optimization problem:

$$\ell = \arg \min_i P_e \quad \forall i \in \{1, 2, \dots, K\} \quad (2)$$

where  $P_e$  is the error probability and  $K$  is the number of samples collected in a symbol time.

In the following, we derive an analytical expression for the error probability, under additive white Gaussian noise (AWGN) and under a fading channel.

#### A. Performance Analysis under AWGN

We first analyse the performance of the proposed UWB receiver under an AWGN channel, since this is the first step towards further analysis under fading channel. Also, we assume that the transmitted pulse shape is a second derivative Gaussian pulse [11]. For the samples received within each symbol duration, two possible hypotheses can be made, namely  $H_0$

and  $H_1$ , corresponding to the source sending a “0” and a “1”, respectively. Specifically,

$$H_0 : r_i = n_i, \quad i = 1, \dots, K, \quad (3)$$

$$H_1 : r_i = \begin{cases} s_i + n_i, & i = 1, \dots, N_p \\ n_i, & i = N_p + 1, \dots, K. \end{cases} \quad (4)$$

In the above definitions,  $s$  is the transmitted pulse,  $r_i$  is the  $i$ -th received sample,  $K$  is the total number of samples received within each symbol time  $T_R$ , and  $N_p$  is the number of samples within a pulse duration  $T_p$ . Hence,  $K = T_R f_s$  and  $N_p = T_p f_s$ , where  $f_s$  is the sampling frequency. For the transmission of a “0”, i.e., hypothesis  $H_0$ , the received samples are noise only, and  $r_i$  follows  $\mathcal{N}(0, \sigma^2)$  where  $\mathcal{N}(a, b)$  denotes the Gaussian distribution with mean  $a$  and variance  $b$ . For the transmission of a “1”, i.e., hypothesis  $H_1$ ,  $r_i$  follows  $\mathcal{N}(s_i, \sigma^2)$ , for  $i \in [1 : N_p]$  and  $\mathcal{N}(0, \sigma^2)$  for  $i \in [N_p + 1 : K]$ . IN is incorporated in the total noise component  $n_i$  according to  $n_i = \tilde{n}_i + z_i$ , where  $\tilde{n}_i$  is the AWGN which follows  $\mathcal{N}(0, \sigma_n^2)$  and  $z_i$  represents the IN, which is modelled as a Bernoulli-Gaussian random variable [7]. We have  $z_i = b_i w_i$  where  $w_i$  follows  $\mathcal{N}(0, \sigma_w^2)$  and  $b_i$  is a Bernoulli random variable with probability mass function

$$\mathbb{P}(b_i) = \begin{cases} \rho, & b_i = 1 \\ 0, & b_i = 0 \end{cases} \quad i = 1, 2, \dots, K. \quad (5)$$

In the above expression,  $\rho$  is the probability of occurrence of IN within a symbol time. The probability density function (pdf) of  $n_i$  is given by [7]

$$f_{n_i}(n_i) = (1 - \rho)\mathcal{G}(n_i, 0, \sigma_n^2) + \rho\mathcal{G}(n_i, 0, \sigma_n^2 + \sigma_w^2), \quad (6)$$

where  $\mathcal{G}(\cdot)$  is the Gaussian pdf. Since  $n_i$  is a weighted sum of two Gaussian-distributed random variables,  $n_i$  follows a Gaussian distribution with zero mean and variance  $\sigma^2 = (1 - \rho)\sigma_n^2 + \rho(\sigma_n^2 + \sigma_w^2)$ , i.e.,  $n_i$  follows  $\mathcal{N}(0, \sigma^2)$ .

Under hypothesis  $H_0$  and  $H_1$ , and denoting with  $\lambda$  the detection threshold, the probability distribution of  $r_i$  is given by:

$$\mathbb{P}(r_i < \lambda | H_0) = F_{H_0} = \frac{1}{2} + \frac{1}{2} \operatorname{erf} \left( \frac{\lambda}{\sqrt{2}\sigma} \right) \quad (7)$$

$$\mathbb{P}(r_i < \lambda | H_1) =$$

$$F_i = \begin{cases} \frac{1}{2} + \frac{1}{2} \operatorname{erf} \left( \frac{\lambda - s_i}{\sqrt{2}\sigma} \right), & i = 1, \dots, N_p \\ \frac{1}{2} + \frac{1}{2} \operatorname{erf} \left( \frac{\lambda}{\sqrt{2}\sigma} \right), & i = N_p + 1, \dots, K. \end{cases} \quad (8)$$

1) *Distribution of  $\ell^{\text{th}}$ -order sample:* The first step performed by the proposed receiver is to sort the received samples according to  $r_{(1)} \leq r_{(2)} \leq \dots \leq r_{(\ell)} \leq \dots \leq r_{(K)}$ . Assuming we use the  $\ell^{\text{th}}$ -order sample  $r_{(\ell)}$ , under  $H_0$  the probability distribution of  $r_{(\ell)}$  is given by the distribution of the ordered version of independent and identically distributed Gaussian random variables [12]:

$$\begin{aligned} \mathbb{P}(r_{(\ell)} < \lambda | H_0) &= G_{H_0} \\ &= \sum_{i=\ell}^K \binom{K}{i} [F_{H_0}]^i [1 - F_{H_0}]^{K-i}. \end{aligned} \quad (9)$$

Under  $H_1$ , instead, the samples are independent but not identically distributed; hence [12],

$$\begin{aligned} \mathbb{P}(r_{(\ell)} < \lambda | H_1) &= G_{H_1} \\ &= \sum_{i=\ell}^K \sum_{B_i} \prod_{j=1}^i F_{c_j} \prod_{j=i+1}^K [1 - F_{c_j}], \end{aligned} \quad (10)$$

where  $B_i$  is a summation that extends over all permutations  $c_1, \dots, c_K$  of  $1, \dots, K$  at which  $(c_1 < \dots < c_i)$  and  $c_{i+1} < \dots < c_K$ .  $G_{H_1}$  takes into consideration all  $K$  samples received under  $H_1$ . Note that, when  $r_{(\ell)} > \lambda$ , this implies that all  $K - \ell + 1$  samples are greater than  $\lambda$ , which increases the confidence that  $H_1$  is detected. When instead  $r_{(\ell)} < \lambda$ ,  $K - \ell + 1$  samples (whose amplitude may be greater than  $\lambda$ ) will be ignored (see also Fig. 1), thus reducing the impact of IN.

2) *Bit error probability*: The error probability can be estimated in terms of the probability of false alarm,  $P_f$ , and of the probability of detection,  $P_d$ . The probability of false alarm indicates the case when the selected sample exceeds the threshold while the transmitted bit is "0". On the contrary, the probability of detection indicates the case where the selected sample exceeds the threshold when the transmitted bit is "1". The probability of error,  $P_e$ , can be written as

$$P_e = (1 - P_d) \times P\{H_1\} + P_f \times P\{H_0\}, \quad (11)$$

where  $P\{H_1\}$  and  $P\{H_0\}$  are the probabilities of  $H_1$  and  $H_0$ , respectively. The probability of false alarm and of detection are given, respectively, by:

$$P_f = \mathbb{P}\{r_{(\ell)} > \lambda | H_0\} = 1 - G_{H_0}, \quad (12)$$

$$P_d = \mathbb{P}\{r_{(\ell)} > \lambda | H_1\} = 1 - G_{H_1}. \quad (13)$$

In the case of a symmetric source, we have:  $P\{H_1\} = P\{H_0\} = 1/2$ , then the error probability becomes:

$$P_e = \frac{1}{2} + \frac{1}{2} \times G_{H_1} - \frac{1}{2} \times G_{H_0}. \quad (14)$$

Substituting (9) and (10) in (14) yields

$$\begin{aligned} P_e &= \frac{1}{2} + \frac{1}{2} \sum_{i=\ell}^K \sum_{B_i} \prod_{j=1}^i F_{c_j} \prod_{j=i+1}^K [1 - F_{c_j}] \\ &\quad - \frac{1}{2} \sum_{i=\ell}^K \binom{K}{i} [F_{H_0}]^i [1 - F_{H_0}]^{K-i}. \end{aligned} \quad (15)$$

As noted in [12], (10) has ensuing complications; hence, we use the approximated recursive method presented in [13] to solve it for  $G_{H_1}$ . For  $\ell = 2, \dots, K$ , we have

$$\begin{aligned} \mathbb{P}(r_{(\ell)} < \lambda | H_1) &= Q_{(\ell)} \\ &= Q_{(\ell-1)} - (1 - Q_{(1)}) V_{(\ell)}, \end{aligned} \quad (16)$$

with

$$Q_{(1)} = 1 - \prod_{i=1}^K 1 - F_i, \quad (17)$$

where  $F_i$  is calculated using (8) and

$$V_{(\ell)} = \frac{1}{\ell - 1} \sum_{i=1}^{\ell-1} (-1)^{i+1} U_i V_{(\ell-i)} \quad (18)$$

with  $V_{(1)} = 1$  and

$$U_{(\ell)} = \sum_{i=1}^K \left( \frac{F_i}{1 - F_i} \right)^\ell. \quad (19)$$

Solving recursively for  $Q_{(\ell)}$  and  $V_{(\ell)}$ ,  $P_e$  can be obtained as

$$\begin{aligned} P_e &= \frac{1}{2} + \frac{1}{2} (Q_{(\ell-1)} - (1 - Q_{(1)}) V_{(\ell)}) \\ &\quad - \frac{1}{2} \sum_{i=\ell}^K \binom{K}{i} [F_{H_0}]^i [1 - F_{H_0}]^{K-i}. \end{aligned} \quad (20)$$

### B. Performance analysis under fading channel

We now extend our analysis to a scenario with fading channel. In this case, the received signal is

$$r(t) = s(t) * h(t) + n(t), \quad (21)$$

where  $h$  is the channel impulse response (CIR) and  $*$  denotes the convolution operator. Under flat fading channel, which is suitable for nonline-of-sight propagation between slowly moving nodes [10],  $h = \alpha \delta(t)$ , where  $\delta(\cdot)$  is the Dirac delta function and  $\alpha$  is the propagation path amplitude. The latter follows a Nakagami- $m$  distribution with pdf [10], [14]:

$$f_{Nak}(\gamma) = \frac{1}{\Gamma(m)} \left( \frac{m}{\bar{\gamma}} \right)^m \gamma^{m-1} \exp\left(-\frac{m\gamma}{\bar{\gamma}}\right), \quad (22)$$

where  $m \geq 0.5$  is the fading parameter,  $\gamma$  is the instantaneous SNR and  $\bar{\gamma}$  is the average instantaneous SNR.  $P_f$  in (12) remains the same under Nakagami- $m$  fading channel. To obtain a closed-form expression for the error probability under Nakagami- $m$  fading channel, we first rewrite the probability distribution under  $H_1$  in (8) in terms of the SNR, which is given by  $\gamma_i = \frac{\alpha^2 s_i^2}{\sigma^2}$ . We get:

$$F_i(\gamma_i) = \begin{cases} \frac{1}{2} + \frac{1}{2} \operatorname{erf}\left(\frac{\frac{\lambda}{\sigma^2} - \gamma_i}{\sqrt{\frac{2}{\sigma^2}}}\right), & i = 1, \dots, N_p \\ \frac{1}{2} + \frac{1}{2} \operatorname{erf}\left(\frac{\lambda}{\sqrt{2}\sigma^2}\right), & i = N_p + 1, \dots, K. \end{cases} \quad (23)$$

The probability distribution of  $r_{(\ell)}$  in (10) is rewritten using (23), which is then substituted in (13) to obtain  $P_d(\gamma_i)$ . The probability of detection under Nakagami- $m$  fading channel is derived by averaging  $P_d(\gamma_i)$  over (22):

$$P_{d_{Nak}} = \int_0^\infty P_d(\gamma_i) f_{Nak}(\gamma_i) d\gamma_i. \quad (24)$$

Hence, the total error probability is given by:

$$\begin{aligned} P_{e_{Nak}} &= \frac{1}{2} + \frac{1}{2} \times \\ &\quad \left( \int_0^\infty \left( \sum_{i=\ell}^K \sum_{B_i} \prod_{j=1}^i F_{c_j}(\gamma_i) \prod_{j=i+1}^K [1 - F_{c_j}(\gamma_i)] \right) \right. \\ &\quad \times \frac{1}{\Gamma(m)} \left( \frac{m}{\bar{\gamma}_i} \right)^m \gamma_i^{m-1} \exp\left(-\frac{m\gamma_i}{\bar{\gamma}_i}\right) d\gamma_i \\ &\quad \left. - \frac{1}{2} \sum_{i=\ell}^K \binom{K}{i} [F_{H_0}]^i [1 - F_{H_0}]^{K-i} \right). \end{aligned} \quad (25)$$

Considering a frequency-selective fading channel, the channel impulse response is defined as

$$h(t) = \sum_{m=1}^M \alpha_m \delta(t - \tau_m), \quad (26)$$

where  $M$  is the number of multipath components (MPC),  $\alpha_m = |\alpha_m|e^{j\theta_m}$  and  $\tau_m$  are the amplitude and time delay of the  $m^{\text{th}}$  path, respectively, and  $\theta_m$  follows a uniform distribution. As per the UWB general channel model in IEEE 802.15.4a [15], the MPCs tend to arrive in clusters with  $\tau_m = T_a + \tau_{a,m}$ , where  $T_a$  is the delay of the  $a^{\text{th}}$  cluster and  $\tau_{a,m}$  is inter-arrival time within a cluster. There exist different models for  $\tau_{a,m}$ , which are uniform, Poisson process and mixed Poisson process [15]. The inter-cluster arrival time also is modelled using a Poisson process. To find a closed-form expression for the error probability under the channel model in (26), one can follow the approach in [10] and average (15) over the distribution of  $\tau_m$ , assuming a fixed channel amplitude  $\alpha_m$ . The resulting expression can then be averaged over the distribution of  $\alpha_m$ , which is a cumbersome process.

### C. Optimization over $\ell$

Given the above expressions for  $P_e$ , the objective function in (2) turns out to be nonlinear with integer decision variable, which makes the optimization problem non-convex. There exist several methods to find the index  $\ell$  minimizing  $P_e$  in this case, however, due to the single integer dimension and the finite set of feasible values, using exhaustive search to find the optimal  $\ell$  is not computationally expensive. In particular, an exhaustive search to find the optimal  $\ell$  can be performed offline. Specifically, the optimal sample index can be computed for each value of signal to noise ratio (SNR) level and saved in a lookup table (LUT), from which it can then be retrieved during the signal detection. We remark that such an approach of estimating a parameter offline and save it in a LUT to be used during deployment has been widely used in the context of UWB system design (see, e.g., [16] where the threshold is estimated through Monte-Carlo simulations for different parameters including SNR, and saved in a LUT to be used later).

## IV. NUMERICAL RESULTS

In this section, we evaluate the performance of the proposed receiver, and validate our analysis against simulation results. Furthermore, we compare the performance against that of existing solutions. To this end, we considered an UWB system with the following parameters: pulse duration = 2 ns, bandwidth  $W = 870$  MHz, and  $f_s = 16$  GHz [3], [6], [17].

### A. Threshold estimation

As done in [5], [18], [19], we set the threshold of our proposed receiver based on a constant false alarm rate (CFAR). In particular, for a fixed  $P_f$ , we solve (12) for the threshold  $\lambda$ . This is very useful when using OOK modulation, since under  $H_0$ , the receiver collects noise-only samples, for which  $P_f$  is well defined by (12), which is also not impacted by the

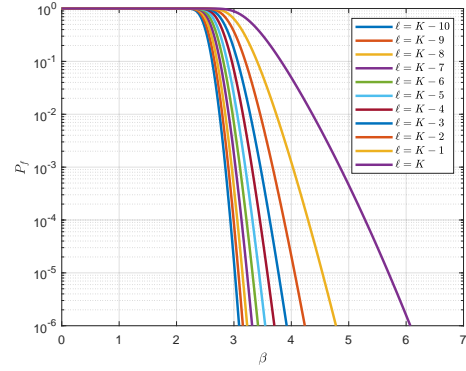


Fig. 2:  $P_f$  vs  $\beta$ , for different values of  $\ell$ .

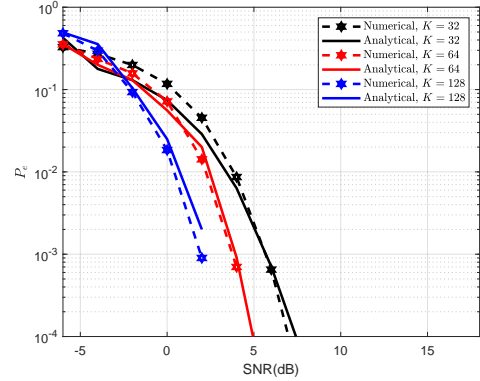


Fig. 3: Numerical vs. analytical results:  $P_e$  as a function of the SNR, for  $K = 32, 64$  and  $128$ .

fading channel. We define  $\lambda = \beta\sigma$ , with  $\sigma$  being the square root of the variance of the distribution of  $r_i$  under  $H_0$ , i.e., the standard deviation, and  $\beta$  is constant. We then use (12) to plot  $P_f$  in Fig. 2, as the value of  $\beta$  varies,  $R = 10$  MHz, and for different values of  $\ell$ . Note that when  $\ell = K$ , the receiver reduces to the single-peak detector, for which the probability of false alarm can be written as [3]:  $P_f = 1 - (F_{H_0})^K$ .

### B. Numerical vs. analytical results

Since the derived error probability under AWGN provides the basis for further derivation under different fading channels, it is important to assess its validity by comparing analytical and simulation results. Fig. 3 depicts the curves obtained using the expression in (20), using also (17) – (19), and leveraging values of  $\ell$  pre-computed through exhaustive search. The error probability is plotted as a function of the SNR, and is compared against numerical results obtained under the aforementioned parameter settings and for a number of samples,  $K$ , equal to 32, 64 and 128. It can be observed that there is an excellent match between our analytical and numerical results.

### C. Simulation under the IEEE 802.15.4a channel

We now compare the performance of the proposed receiver to the single-peak and the ED receivers, under the standardized UWB IEEE 802.15.4a channel model (CM) [15]. We use CM9, which corresponds to an industrial non-line of sight harsh environment, since IN is more likely to occur in such

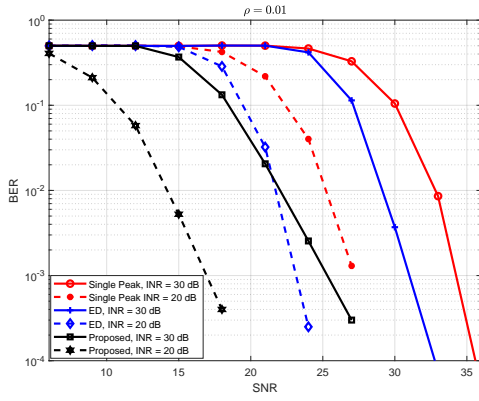


Fig. 4: Bit error probability for the proposed receiver, ED, and single peak vs. SNR, for  $\rho = 0.01$  and  $INR = 20, 301, \text{ dB}$ .

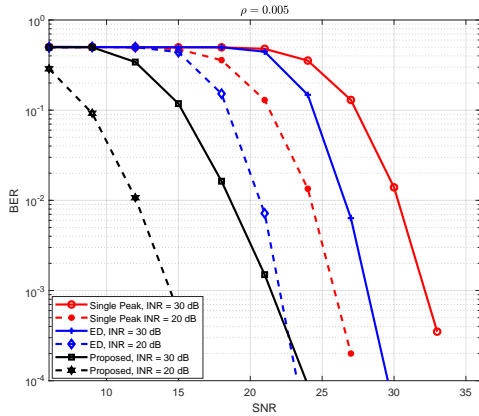


Fig. 5: Bit error probability for the proposed receiver, ED, and single peak vs. SNR, for  $\rho = 0.005$  and  $INR = 20, 30 \text{ dB}$ .

a scenario [4]. The parameters characterizing the simulated channel can be found in [15].

We define  $SNR = \frac{|h|^2 s^2}{\sigma_n^2}$ , IN to noise ratio (INR) as  $INR = \frac{\sigma_w^2}{\sigma_n^2}$ , and signal to IN plus noise ratio (SINR) as  $SINR = \frac{|h|^2 s^2}{(1-\rho)\sigma_n^2 + \rho(\sigma_n^2 + \sigma_w^2)}$ , with  $\rho = \frac{N_I}{K}$ . In the later,  $N_I$  represents the number of IN samples within a symbol time. For the proposed receiver and for single-peak detection [3], the received samples within a symbol time are first sorted in ascending order. Also, for our receiver, we estimate offline (through exhaustive search) the  $\ell$  values that provide the lowest bit error probability under CM9 realizations. We save the optimal  $\ell$  in a LUT and then we compare the selected sample to the threshold. For single-peak detection, instead, the sample with the maximum value, i.e.,  $\ell = K$ , is selected and compared to the threshold. Finally, for ED, the energy of the collected samples within each symbol time is estimated and then compared to the threshold.

Figures 4 and 5 present the bit error rate (BER) at  $R = 10$  MHz for all considered receivers, when  $\rho = 0.01$  and  $0.005$ , respectively. We consider both  $INR = 30 \text{ dB}$  and  $INR = 20 \text{ dB}$ . The proposed receiver significantly outperforms both single-peak and ED receivers. For example, for  $\rho = 0.01$  and BER of  $10^{-3}$ , our receiver requires  $SNR \approx 25 \text{ dB}$ , while single peak and ED require  $SNR = 31$  and  $34 \text{ dB}$ , respectively. Overall, our solution improves the dynamic range of the

receiver by an average of 5–10 dB when compared to ED and single peak. Another way to look at these results is for a fixed SNR: the proposed receiver can reduce the BER by orders of magnitude compared to the considered benchmarks. At last, the performance of all receivers improve when either  $\rho$  or  $INR$  decreases.

## V. CONCLUSION

We presented a non-coherent, threshold-based UWB receiver that leverages a single sample, namely, the  $\ell^{\text{th}}$ -order sample. We analytically derived a closed-form expression for the bit error probability and assessed the performance of our solution through numerical results in a IEEE 802.15.4a scenario. The results show that, in the presence of IN, the proposed receiver improves by multiple orders of magnitude the detection performance of existing, non-coherent UWB receivers.

## REFERENCES

- [1] F. Wang, Z. Tian, and B. M. Sadler, "Weighted energy detection for noncoherent ultra-wideband receiver design," *IEEE Trans. on Wireless Communications*, vol. 10, no. 2, pp. 710–720, February 2011.
- [2] A. A. D'Amico, U. Mengali, and E. A. de Reyna, "Energy-detection uwb receivers with multiple energy measurements," *IEEE Trans. on Wireless Communications*, vol. 6, no. 7, pp. 2652–2659, July 2007.
- [3] K. Allidina, T. Khattab, and M. N. El-Gamal, "On dual peak detection UWB receivers in noise and interference dominated environments," *AEU International Journal of Electronics and Communications*, vol. 70, no. 2, pp. 121 – 131, 2016.
- [4] M. Cheffena, "Propagation channel characteristics of industrial wireless sensor networks [wireless corner]," *IEEE Antennas and Propagation Magazine*, vol. 58, no. 1, pp. 66–73, Feb 2016.
- [5] H. Ding, W. Liu, X. Huang, and L. Zheng, "First path detection using rank test in ir uwb ranging with energy detection receiver under harsh environments," *IEEE Communications Letters*, vol. 17, no. 4, pp. 761–764, April 2013.
- [6] S. Sharma, V. Bhatia, K. Deka, and A. Gupta, "Sparsity-based monobit uwb receiver under impulse noise environments," *IEEE Wireless Communications Letters*, vol. 8, no. 3, pp. 849–852, June 2019.
- [7] K. M. Rabie and E. Alsusa, "Preprocessing-based impulsive noise reduction for power-line communications," *IEEE Transactions on Power Delivery*, vol. 29, no. 4, pp. 1648–1658, Aug 2014.
- [8] S. Niranjayan and N. C. Beaulieu, "Novel adaptive nonlinear receivers for uwb multiple access communications," *IEEE Transactions on Wireless Communications*, vol. 12, no. 5, pp. 2014–2023, May 2013.
- [9] S. Sharma, A. Gupta, and V. Bhatia, "Impulse noise mitigation in ir-ubw communication using signal cluster sparsity," *IEEE Communications Letters*, vol. 22, no. 3, pp. 558–561, March 2018.
- [10] A. Giorgetti, M. Chiani, and M. Win, "The effect of narrowband interference on wideband wireless communication systems," *IEEE Transactions on Communications*, vol. 53, no. 12, pp. 2139–2149, Dec 2005.
- [11] H. Arslan, Z. N. Chen, and M.-G. Di Benedetto, *Ultra wideband wireless communication*. John Wiley & Sons, 2006.
- [12] H. David and H. Nagaraja, *Order Statistics*, ser. Wiley Series in Probability and Statistics.
- [13] G. Cao and M. West, "Computing distributions of order statistics," *Communications in Statistics - Theory and Methods*, vol. 26, no. 3, pp. 755–764, 1997.
- [14] D. Horgan and C. C. Murphy, "Fast and accurate approximations for the analysis of energy detection in nakagami-m channels," *IEEE Communications Letters*, vol. 17, no. 1, pp. 83–86, January 2013.
- [15] A. F. Molisch, D. Cassioli, C. Chong, S. Emami, A. Fort, B. Kannan, J. Karedal, J. Kunisch, H. G. Schantz, K. Siwiak, and M. Z. Win, "A comprehensive standardized model for ultrawideband propagation channels," *IEEE Transactions on Antennas and Propagation*, vol. 54, no. 11, pp. 3151–3166, Nov 2006.
- [16] V. Kristem, A. F. Molisch, S. Niranjayan, and S. Sangodoyin, "Coherent uwb ranging in the presence of multiuser interference," *IEEE Transactions on Wireless Communications*, vol. 13, no. 8, pp. 4424–4439, Aug 2014.

- [17] S. Sharma, V. Bhatia, and A. Gupta, "Joint symbol and toa estimation for iterative transmitted reference pulse cluster uwb system," *IEEE Systems Journal*, vol. 13, no. 3, pp. 2629–2640, Sep. 2019.
- [18] D. Dardari, C. Chong, and M. Win, "Threshold-based time-of-arrival estimators in uwb dense multipath channels," *IEEE Transactions on Communications*, vol. 56, no. 8, pp. 1366–1378, August 2008.
- [19] A. Maali, A. Mesloub, M. Djeddou, H. Mimoun, G. Baudoin, and A. Ouldali, "Adaptive ca-cfar threshold for non-coherent ir-uwb energy detector receivers," *IEEE Communications Letters*, vol. 13, no. 12, pp. 959–961, December 2009.